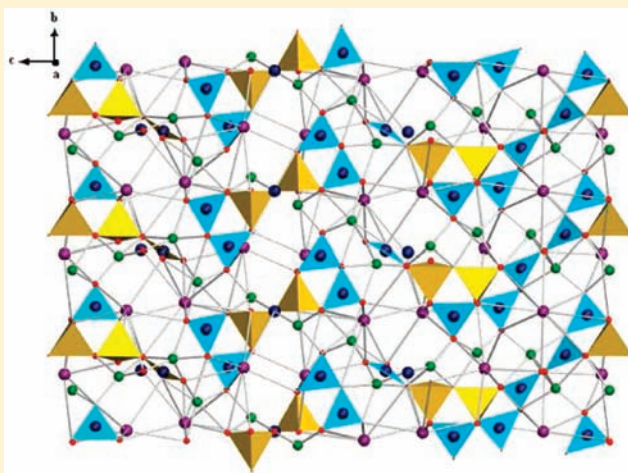


Li₄Cs₃B₇O₁₄: Synthesis, Crystal Structure, and Optical Properties

Yun Yang,^{†,‡} Shilie Pan,^{†,*} Hongyi Li,[†] Jian Han,[†] Zhaohui Chen,^{†,‡} Wenwu Zhao,^{†,‡} and Zhongxiang Zhou[†][†]Xinjiang Key Laboratory of Electronic Information Materials and Devices, Xinjiang Technical Institute of Physics & Chemistry, Chinese Academy of Sciences, 40-1 South Beijing Road, Urumqi 830011, China[‡]Graduate School of the Chinese Academy of Sciences, Beijing 100039, PR China and College of Chemistry and Chemical Engineering

S Supporting Information

ABSTRACT: A new noncentrosymmetric polyborate, Li₄Cs₃B₇O₁₄, has been synthesized using the conventional solid state reaction method. It crystallizes in the trigonal space group *P3₁21* (No. 152) with unit cell parameters of *a* = 6.9313(6) Å, *c* = 26.799(3) Å, and *Z* = 3. The new structure contains an infinite three-dimensional matrix that is built from B₇O₁₄ building blocks rarely found in anhydrous borate compounds and LiO_{*n*} (*n* = 4, 5), CsO_{*n*} (*n* = 9, 10) polyhedra. The optical characterization of the compound indicates that the compound is phase matchable, and the UV cutoff edge is below 190 nm. IR spectroscopy, thermal analysis, and second-harmonic generation were also performed on the reported material.



INTRODUCTION

Nonlinear optical (NLO) materials have long been a remarkable focus of research projects, especially borate crystals,^{1–19} for their variety of noncentrosymmetric structure types, transparency to a wide range of wavelengths, high damage threshold, and high optical quality.^{11c} Even though much effort has focused on the design and controlled synthesis of new NLO materials with enhanced merits over the last two decades, it is still a great challenge to design new materials with a preset function by an inorganic crystal engineering method. Research on NLO materials reveals that borate compounds are superior to other commonly used NLO materials for UV applications.^{8a} The design and construction of new inorganic NLO materials often utilize B–O fundamental building blocks. A variety of B–O groups are considered to be a dominant factor in their physical properties, in particular the optical properties of borates.^{1f} In addition, the alkali metal–oxygen bond is ideal for the transmission of UV light because there are no electron transitions in this range.^{1e} Among the alkali metal borate NLO materials designed, several crystals can produce UV coherent light, such as LiB₃O₅ (LBO),^{2a} CsB₃O₅ (CBO),^{3a} and CsLiB₆O₁₀ (CLBO),^{4a} etc. The excellent properties of alkali metal borates inspire us to explore new NLO materials in borate systems.²⁰

In this study, we carried out systematic explorations on the Li₂O–Cs₂O–B₂O₃ ternary system to expand and codify the structural chemistry of mixed alkali–metal borates and identify novel materials. A new noncentrosymmetric polyborate,

Li₄Cs₃B₇O₁₄, with a UV cutoff wavelength below 190 nm was found, and it consists of the B₇O₁₄ fundamental building block, which is rarely found in an anhydrous borate compound.²¹ The synthesis, structure, thermal behavior, spectrum, and optical properties of the borate are described in this paper.

EXPERIMENTAL SECTION

Reagent. All commercially available chemicals (Li₂CO₃, Cs₂CO₃, and H₃BO₃) are of reagent grade and were used as received.

Crystal Growth. Small single crystals of Li₄Cs₃B₁₀O₁₇ were grown by melting a mixture of Li₂CO₃, Cs₂CO₃, and H₃BO₃ with a 2:3:10 molar ratio at 800 °C in a platinum crucible that was placed into a vertical, programmable temperature furnace. It was held at that temperature for 24 h, then slowly cooled to 630 °C at a rate of 0.05 °C/min, and finally cooled to room temperature at a rate of 10 °C/min. Colorless block crystals were separated from the crucible for structural characterization with 15% yield (based on Cs). Crystals suitable for X-ray diffraction were selected under an optical microscope. Crystal picture of Li₄Cs₃B₁₀O₁₇ is shown in Figure 1.

Solid-State Synthesis. Polycrystalline samples of Li₄Cs₃B₇O₁₄ were synthesized via solid-state reactions from mixtures of Li₂CO₃, Cs₂CO₃, and H₃BO₃ as the starting components in a molar ratio of 4:3:14. The sample was heated to 560 °C slowly and held at this temperature for 48 h with several intermediate grindings and mixings.

Received: November 4, 2010

Published: February 21, 2011

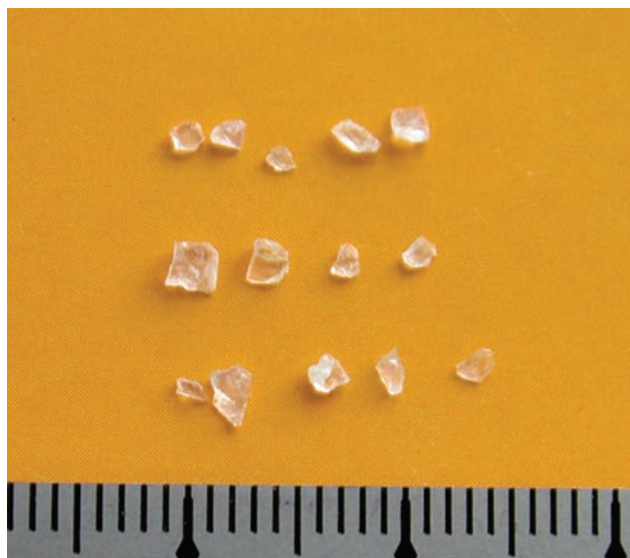


Figure 1. Photograph of $\text{Li}_4\text{Cs}_3\text{B}_7\text{O}_{14}$ crystals. (The minimum scale of the ruler is one millimeter.)

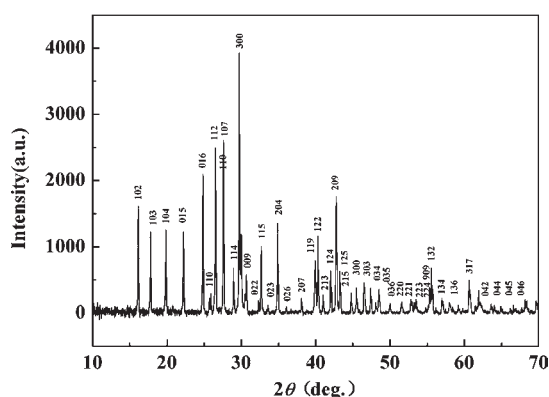


Figure 2. Powder XRD pattern of $\text{Li}_4\text{Cs}_3\text{B}_7\text{O}_{14}$.

The purity of the sample was checked by XRD diffraction, as shown in Figure 2. The XRD measurements on $\text{Li}_4\text{Cs}_3\text{B}_7\text{O}_{14}$ were performed at room temperature on a Bruker D8 ADVANCE X-ray diffractometer with graphite monochromatized $\text{Cu K}\alpha$ ($\lambda = 1.5418 \text{ \AA}$) radiation. The diffraction patterns were taken from 10° to 70° (2θ). The measured XRD powder pattern matches the one simulated from single-crystal X-ray diffraction studies (Figure S1 of the Supporting Information).

Structure Determination. The crystal structure of $\text{Li}_4\text{Cs}_3\text{B}_7\text{O}_{14}$ was investigated by single-crystal X-ray diffraction on a Bruker SMART APEX II CCD diffractometer using monochromatic $\text{Mo K}\alpha$ radiation ($\lambda = 0.71073 \text{ \AA}$) at $293(2) \text{ K}$ and integrated with the SAINT program.²² All calculations were performed with programs from the SHELXTL crystallographic software package.²³ The structure was solved by direct methods using SHELXS-97.²⁴ Final least-squares refinement is on F_o^2 with data having $F_o^2 \geq 2\sigma(F_o^2)$. It was checked for missing symmetry elements with PLATON.²⁵ Crystal data and structure refinement information are summarized in Table 1. The final refined atomic positions and isotropic thermal parameters are given in Table 2. The main interatomic distances and angles are listed in Table S1 of the Supporting Information.

Vibrational Spectroscopy. IR spectroscopy was carried out with the objective of specifying and comparing the coordination of boron in $\text{Li}_4\text{Cs}_3\text{B}_7\text{O}_{14}$. The mid-infrared spectrum was obtained at room temperature via a Bio-Rad FTS-60 FTIR spectrometer. The sample was

Table 1. Crystal Data and Structure Refinement for $\text{Li}_4\text{Cs}_3\text{B}_7\text{O}_{14}$

empirical formula	$\text{B}_7\text{Cs}_3\text{Li}_4\text{O}_{14}$
temperature	293(2)
formula weight	726.16
crystal system	trigonal
space group	$P3_121$
unit cell dimensions	$a = 6.9313(6) \text{ \AA}$ $c = 26.799(3) \text{ \AA}$
volume	$1115.01(19) \text{ \AA}^3$
Z	3
density (calculated)	3.244 g/cm^3
absorption coefficient	$7.386/\text{mm}$
$F(000)$	972
crystal size	$0.21 \times 0.18 \times 0.05 \text{ mm}^3$
theta range for data collection	$3.39\text{--}27.41^\circ$
index ranges	$-8 \leq h \leq 8, -8 \leq k \leq 8, -34 \leq l \leq 33$
reflections collected/unique	8384/1310 [$R(\text{int}) = 0.1731$]
completeness to theta = 27.41	99.9%
refinement method	full-matrix least-squares on F^2
data/restraints/parameters	1310/0/130
goodness-of-fit on F^2	0.990
final R indices [$F_o^2 > 2\sigma(F_o^2)$] ^a	$R1 = 0.0403, wR2 = 0.0704$
R indices (all data) ^a	$R1 = 0.0550, wR2 = 0.0735$
largest diff. peak and hole	0.966 and $-1.484 \text{ e \AA}^{-3}$
flack parameter	$-0.06(4)$

$$^a R_1 = \frac{\sum ||F_o| - |F_c||}{\sum |F_o|} \text{ and } wR_2 = \frac{[\sum w(F_o^2 - F_c^2)^2 / \sum w F_o^4]^{1/2}}{2} \text{ for } F_o^2 > 2\sigma(F_o^2).$$

Table 2. Atomic Coordinates ($\times 10^4$) and Equivalent Isotropic Displacement Parameters ($\text{\AA}^2 \times 10^3$) for $\text{Li}_4\text{Cs}_3\text{B}_7\text{O}_{14}$ ^a

atom	x	y	z	U_{eq}
Cs(1)	5321(1)	10084(1)	1089(1)	24(1)
Cs(2)	734(1)	10734(1)	0	31(1)
O(1)	10007(10)	9318(8)	1221(1)	22(1)
O(2)	3474(7)	5035(9)	774(1)	18(1)
O(3)	10000	12271(11)	1667	24(2)
O(4)	-107(7)	6209(8)	789(1)	16(1)
O(5)	6681(8)	5793(10)	1243(1)	25(1)
O(6)	4235(9)	9229(9)	-29(1)	18(1)
O(7)	10000	6294(10)	1667	19(2)
O(8)	6267(8)	4420(9)	421(1)	18(1)
B(1)	5357(12)	5102(13)	816(3)	13(2)
B(2)	9126(13)	6919(15)	1235(2)	17(2)
B(3)	10000	10387(16)	1667	15(2)
B(4)	8503(14)	14961(14)	401(2)	16(2)
Li(1)	11150(20)	14580(20)	1234(4)	20(3)
Li(2)	2456(18)	6045(17)	230(3)	12(2)

^a U_{Eq} is defined as one-third of the trace of the orthogonalized U_{ij} tensor.

mixed thoroughly with dried KBr (5 mg of the sample, 500 mg of KBr). It was collected in a range from 400 to 4000 cm^{-1} with a resolution of 1 cm^{-1} .

Differential Thermal Analysis. Thermal analysis was carried out on NETZSCH STA 449C instrument at a temperature range of $30\text{--}900 \text{ }^\circ\text{C}$ with a heating rate of $10 \text{ }^\circ\text{C}/\text{min}$ in an atmosphere of flowing N_2 .

Elemental Analysis. Elemental analysis of $\text{Li}_4\text{Cs}_3\text{B}_7\text{O}_{14}$ single crystal was measured by using a VISTA-PRO CCD Simultaneous ICP-OES. The crystal samples were dissolved in nitric acid at boiling point for 1 h. Anal. Calcd for the $\text{Li}_4\text{Cs}_3\text{B}_7\text{O}_{14}$: Li, 3.82; Cs, 54.91; B, 10.42. Found: Li, 4.05; Cs, 54.72; B, 10.47.

UV-vis-NIR Diffuse Reflectance Spectroscopy. UV-vis-NIR diffuse reflectance of $\text{Li}_4\text{Cs}_3\text{B}_7\text{O}_{14}$ crystalline samples was collected with a

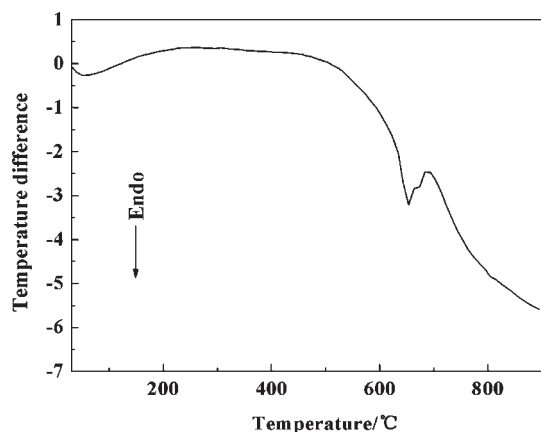


Figure 3. DTA curve of $\text{Li}_4\text{Cs}_3\text{B}_7\text{O}_{14}$.

SolidSpec-3700DUV spectrophotometer using fluoro-resin as a standard in the wavelength range from 190 to 2600 nm.

NLO Measurements. Powder second-harmonic generation (SHG) tests were carried out on $\text{Li}_4\text{Cs}_3\text{B}_7\text{O}_{14}$ by the Kurtz–Perry method using 1064 nm radiation.²⁶ A detailed description of the equipment and the methodology used has been published.¹⁷

RESULTS AND DISCUSSION

Thermal Behavior. Figure 3 presents the DTA curve of $\text{Li}_4\text{Cs}_3\text{B}_7\text{O}_{14}$. There are two endothermic peaks as the sample being heated, which suggests that $\text{Li}_4\text{Cs}_3\text{B}_7\text{O}_{14}$ melts incongruently. The two endothermic peaks begin at 654 and 672 °C, respectively. In order to further verify that $\text{Li}_4\text{Cs}_3\text{B}_7\text{O}_{14}$ melts incongruently, 0.5 g of $\text{Li}_4\text{Cs}_3\text{B}_7\text{O}_{14}$ powder was packed into a platinum crucible, heated to 900 °C, and then rapidly cooled to room temperature. Analysis of the powder XRD pattern of the solidified melt revealed that the entire solid product exhibited a diffraction pattern different from that of the initial $\text{Li}_4\text{Cs}_3\text{B}_7\text{O}_{14}$ powder (Figure S2 of the Supporting Information), further demonstrating that $\text{Li}_4\text{Cs}_3\text{B}_7\text{O}_{14}$ is an incongruently melting compound. Therefore, the flux method is necessary for the purpose of its crystal growth, and it can be obtained using $\text{Cs}_2\text{O}-\text{B}_2\text{O}_3$ as the flux. The molar ratio of $\text{Li}_4\text{Cs}_3\text{B}_7\text{O}_{14}:\text{Cs}_2\text{O}:\text{B}_2\text{O}_3$ is 1:1.5:1.5.

Crystal Structure. Crystallographic analysis revealed that $\text{Li}_4\text{Cs}_3\text{B}_7\text{O}_{14}$ belongs to the space group $P3_121$. Two unique lithium atoms, two unique cesium atoms, four unique boron atoms, and eight unique oxygen atoms are in an asymmetric unit (Table 2). The structure of $\text{Li}_4\text{Cs}_3\text{B}_7\text{O}_{14}$ features a complicated three-dimensional (3-D) network composed of isolated B_7O_{14} units interconnected by LiO_n ($n = 4, 5$), CsO_n ($n = 9, 10$) distorted polyhedra (Figure 4 and Figure S3 of the Supporting Information). A notable feature in $\text{Li}_4\text{Cs}_3\text{B}_7\text{O}_{14}$ is the B_7O_{14} heptaborate group, consisting of three six-membered rings in which five trigonal BO_3 units and two tetrahedral BO_4 units are linked by vertical oxygen atoms (Figure 4). The dihedral angles between two neighboring B_3O_6 rings in the B_7O_{14} cluster are 72.6° and 107.4°, respectively. According to the classification of polyborate anions proposed by Christ and Clark,¹⁰ the fundamental building blocks shorthand notation for B_7O_{14} in $\text{Li}_4\text{Cs}_3\text{B}_7\text{O}_{14}$ is $7:[5\Delta + 2T]$. Such a polyborate anion with seven boron atoms has only been found in $\text{KBa}_7\text{Mg}_2\text{B}_{14}\text{O}_{28}\text{F}_5$ ²¹ previously in anhydrous borates. The triangularly coordinated boron atoms have B–O distances in the range 1.288(9)–1.428(9) Å [$\text{av} = 1.371$ Å], and the tetrahedral B atoms have longer B–O distances in the range of 1.458(9)–1.488(8) Å

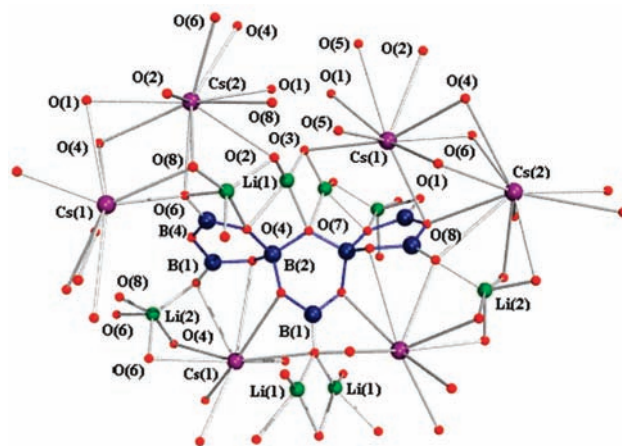


Figure 4. View of the structure of $\text{Li}_4\text{Cs}_3\text{B}_7\text{O}_{14}$ and cations coordinate environments.

[$\text{av} = 1.471$ Å]. These values are comparable to those in other borate compounds reported previously.¹⁷

Each B_7O_{14} group is connected to 14 different CsO_n ($n = 9, 10$) polyhedra, in which there are eight $\text{Cs}(1)\text{O}_9$ and six $\text{Cs}(2)\text{O}_{10}$ polyhedra. The average distances of Cs–O is 3.3482 Å with ranges of 2.939(4)–3.604(6) Å [$\text{av} = 3.3068$ Å] of $\text{Cs}(1)$ and 3.085(5)–3.581(4) Å [$\text{av} = 3.3896$ Å] of $\text{Cs}(2)$. $\text{Cs}(1)\text{O}_9$ and $\text{Cs}(2)\text{O}_{10}$ polyhedra are interconnected by shared oxygen atoms to form the 3-D framework (Figure S4 of the Supporting Information). $\text{Li}(1)$ and $\text{Li}(2)$ atoms are located between the B_7O_{14} and CsO_n ($n = 9, 10$) groups to hold the groups through coordination with oxygen atoms (Figure 4). Each $\text{Li}(1)$ atom is coordinated to four O atoms forming a distorted tetrahedron arrangement with Li–O bond distances ranging from 1.808(13) to 2.108(12) Å [$\text{av} = 1.981$ Å]. Each $\text{Li}(2)$ atom is surrounded by five O atoms forming a trigonal bipyramid with bond distances ranging from 1.899(11) to 2.369(11) Å [$\text{av} = 2.099$ Å]. $\text{Li}(1)\text{O}_5$ and $\text{Li}(2)\text{O}_4$ polyhedra are interconnected via sharing edges into a 3-D framework (Figure S5 of the Supporting Information).

The bond valence sums of each atom in $\text{Li}_4\text{Cs}_3\text{B}_7\text{O}_{14}$ were calculated^{27,28} and are listed in Table S2 of Supporting Information. These valence sums agree with expected oxidation states.

IR Spectroscopy. The spectrum exhibited the following absorptions, which were assigned referring to the literature (Figure S6 of the Supporting Information).^{29–31} The main infrared absorption region between about 1460–1300 cm^{-1} reveals several absorption bands due to the asymmetric stretching of trigonal BO_3 (1458 and 1421 cm^{-1}) groups. The bands at 1129 and 1165 cm^{-1} are the in-plane bending of B–O in BO_3 . The band at 934 cm^{-1} is the symmetric stretching of B–O in BO_3 . The bands at 766, 728, 679, and 635 cm^{-1} are the out-of-plane bending of B–O in BO_3 . The wave numbers of fundamental vibrations of the BO_4 group are grouped into three distinct regions, i.e., 1150–1000, 890–740, and 590–510 cm^{-1} , assigned as the asymmetric stretching (1090 cm^{-1}), symmetric stretching (828 cm^{-1}), and the bending modes (579 cm^{-1}), respectively. $\text{Li}_4\text{Cs}_3\text{B}_7\text{O}_{14}$ is moisture sensitive,³² which is shown from the band at 3428 cm^{-1} .

UV–vis-NIR Diffuse Reflectance Spectroscopy. UV–vis-NIR diffuse reflectance spectrum of $\text{Li}_4\text{Cs}_3\text{B}_7\text{O}_{14}$ crystalline sample is shown in Figure 5. It has a cutoff edge below 190 nm, indicating that the crystal may have potential use in UV NLO applications.

NLO Measurements. On the basis of the noncentrosymmetric crystal structure of $\text{Li}_4\text{Cs}_3\text{B}_7\text{O}_{14}$, it is expected to possess

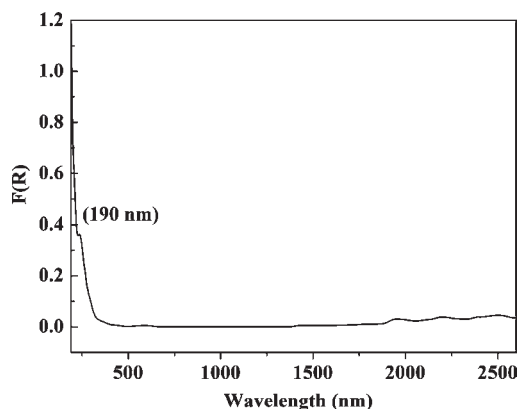


Figure 5. UV-vis-NIR diffuse reflectance spectrum of $\text{Li}_4\text{Cs}_3\text{B}_7\text{O}_{14}$.

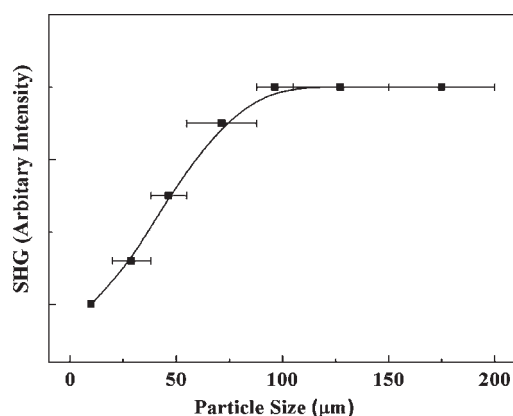


Figure 6. Phase-matching curve, that is, particle size vs SHG intensity for $\text{Li}_4\text{Cs}_3\text{B}_7\text{O}_{14}$. Curve drawn is a guide to the eye and is not a fit to the data.

NLO properties. According to the anionic group theory of NLO activity in borates,³³ the BO_3 trigonal planes are responsible for the large SHG effects, and the BO_4 groups contribute less. Also, the different orientations of the structure limit their total NLO contribution. The angles between two neighboring B_3O_6 rings in B_7O_{14} are 72.6° and 107.4° , respectively, which indicate that each two hexagonal rings are almost perpendicular to each other in this unit. The arrangement of the fundamental building blocks is in an unfavorable manner so that the SHG coefficients are almost canceled. Then, the resulting SHG effects are very limited.³⁴ Consequently, the overall SHG efficiency of $\text{Li}_4\text{Cs}_3\text{B}_7\text{O}_{14}$ is merely about 1/2 KDP. The SHG measurements on the sieved $\text{Li}_4\text{Cs}_3\text{B}_7\text{O}_{14}$ sample indicate that it is phase matchable (Figure 6).

CONCLUSION

With the combination of the alkali metal cation, which can form the alkali metal–oxygen bond with no electron transitions in UV range, and the heptaborate building block, a new UV NLO material, $\text{Li}_4\text{Cs}_3\text{B}_7\text{O}_{14}$, has been prepared. It was obtained by spontaneous crystallization with flux on the basis of the $\text{Cs}_2\text{O}-\text{B}_2\text{O}_3$ solvent. The three-dimensional network consists of isolated heptaborate units B_7O_{14} linked by LiO_n ($n = 4, 5$) and CsO_n ($n = 9, 10$) distorted polyhedra. The UV-vis-NIR diffuse reflectance spectroscopy on powder samples indicates that it has a wide transparent region with the short-wavelength absorption edge below 190 nm. The feature of a short UV cutoff edge is favorable in practical applications. Future efforts will be devoted to the growth of large crystals

and related physical property studies for this compound. Other similar systems leading to new NLO materials are also on the way.

ASSOCIATED CONTENT

S Supporting Information. CIF file; tables of bond valences, bond distances, and angles; and figures of powder X-ray diffraction and infrared spectroscopy. This material is available free of charge via the Internet at <http://pubs.acs.org>.

AUTHOR INFORMATION

Corresponding Author

*Phone: (86)991-3674558. Fax: (86)991-3838957. E-mail: slpan@ms.xjb.ac.cn.

ACKNOWLEDGMENT

This work is supported by the Main Direction Program of Knowledge Innovation of Chinese Academy of Sciences (Grant KJCX2-EW-H03-03), National Natural Science Foundation of China (Grant 50802110, 21001114), One Hundred Talents Project Foundation Program of Chinese Academy of Sciences, Western Light Joint Scholar Foundation Program of Chinese Academy of Sciences, Scientific Research Foundation for the Returned Overseas Chinese Scholars, State Education Ministry (Grant 20091001), and High Technology Research and Development Program of Xinjiang Uygur Autonomous Region of China (Grant 200816120).

REFERENCES

- (1) (a) Chen, C. T.; Wu, B. C.; Jiang, A. D.; You, G. M. *Sci. Sin.* **1985**, *28*, 235. (b) Chen, C. T.; Liu, G. *Annu. Rev. Mater. Sci.* **1986**, *16*, 203. (c) Chen, C. T.; Wu, Y. C.; Li, R. K. *Int. Rev. Phys. Chem.* **1989**, *8*, 65. (d) Chen, C. T.; Wang, Y. B.; Xia, Y. N.; Wu, B. C.; Tang, O. Y.; Wu, K.; Zeng, W.; Yu, L. H. *J. Appl. Phys.* **1995**, *77*, 2268. (e) Chen, C. T.; Wang, Y. B.; Wu, B. C.; Wu, K. W.; Yu, L. H. *Nature* **1995**, *373*, 322. (f) Chen, C. T.; Lin, Z. S.; Wang, Z. *Appl. Phys. B: Laser Opt.* **2005**, *80*, 1. (g) David, C. *Nature* **2009**, *457*, 953.
- (2) (a) Chen, C. T.; Wu, Y. C.; Jiang, A. D.; You, G. M.; Li, R. K.; Lin, S. J. *J. Opt. Soc. Am. B* **1989**, *6*, 616. (b) Bétourné, E.; Touboul, M. *J. Alloys Compd.* **1997**, *255*, 91.
- (3) (a) Wu, Y. C.; Sasaki, T.; Nakai, S.; Yokotani, A.; Tang, H.; Chen, C. T. *Appl. Phys. Lett.* **1993**, *62*, 2614. (b) Touboul, M.; Penin, N.; Nowogrocki, G. *J. Solid State Chem.* **1999**, *143*, 260.
- (4) (a) Mori, Y.; Kuroda, I.; Nakajima, S.; Sasaki, T.; Nakai, S. *Appl. Phys. Lett.* **1995**, *67*, 1818. (b) Tu, J. M.; Keszlér, D. A. *Mater. Res. Bull.* **1995**, *30*, 209. (c) Sasaki, T.; Kuroda, I.; Nakajima, S.; Yamaguchi, K.; Watanabe, S.; Mori, Y.; Nakai, S. Proceedings of the Advanced Solid-State Laser Conference, Memphis, TN, 1995.
- (5) (a) Muller, E. A.; Cannon, R. J.; Sarjeant, A. N.; Ok, K. M.; Halasyamani, P. S.; Norquist, A. J. *Cryst. Growth Des.* **2005**, *5*, 1913. (b) Halasyamani, P. S.; O'Hare, D. *Chem. Mater.* **1998**, *10*, 646. (c) Halasyamani, P. S.; Francis, R. J.; Walker, S. M.; O'Hare, D. *Inorg. Chem.* **1999**, *38*, 271. (d) Halasyamani, P. S.; Poeppelmeier, K. R. *Chem. Mater.* **1998**, *10*, 2753.
- (6) (a) Halasyamani, P. S.; Poeppelmeier, K. R. *Inorg. Chem.* **2008**, *47*, 8427. (b) Pan, S. L.; Smit, J. P.; Marvel, M. R.; Stamper, E. S.; Haag, J. M.; Baek, J.; Halasyamani, P. S.; Poeppelmeier, K. R. *J. Solid State Chem.* **2008**, *181*, 2087. (c) Hagerman, M. E.; Poeppelmeier, K. R. *Chem. Mater.* **1995**, *7*, 602. (d) Maggard, P. A.; Stern, C. L.; Poeppelmeier, K. R. *J. Am. Chem. Soc.* **2001**, *123*, 7742. (e) Pan, S. L.; Smit, J. P.; Watkins, B.; Marvel, M. R.; Stern, C. L.; Poeppelmeier, K. R. *J. Am. Chem. Soc.* **2006**, *128*, 11631.

- (7) (a) Leonyuk, N. I.; Wang, J.; Dawes, J. M.; Kuleshov, N. V. *J. Mater. Sci: Mater. Electron* **2007**, *18*, 293. (b) Rong, C.; Yu, Z. W.; Wang, Q.; Zheng, S. T.; Pan, C. Y.; Deng, F.; Yang, G. Y. *Inorg. Chem.* **2009**, *48*, 3650. (c) Wang, G. M.; Sun, Y. Q.; Yang, G. Y. *J. Solid State Chem.* **2006**, *179*, 398.
- (8) (a) Becker, P. *Adv. Mater.* **1998**, *10*, 979. (b) Becker, P.; Bohaty, L.; Froehlich, R. *Acta Cryst. C* **1995**, *51*, 1721.
- (9) (a) Zhang, W. L.; Chen, W. D.; Zhang, H.; Geng, L.; Lin, C. S.; He, Z. Z. *J. Am. Chem. Soc.* **2010**, *132*, 1508. (b) Mao, J. G.; Jiang, H. L.; Fang, K. *Inorg. Chem.* **2008**, *47*, 8498. (c) Kong, F.; Huang, S. P.; Sun, Z. M.; Mao, J. G.; Cheng, W. D. *J. Am. Chem. Soc.* **2006**, *128*, 7750. (d) Wang, S. C.; Ye, N.; Li, W.; Zhao, D. *J. Am. Chem. Soc.* **2010**, *132*, 8779.
- (10) (a) Christ, C. L.; Clark, J. R. *Phys. Chem. Miner.* **1977**, *2*, 59. (b) Burns, P. C.; Grice, J. D.; Hawthorne, F. C. *Can. Mineral.* **1995**, *33*, 1131. (c) Grice, J. D.; Burns, P. C.; Hawthorne, F. C. *Can. Mineral.* **1999**, *37*, 731. (d) Heller, G. *Top. Curr. Chem.* **1986**, *131*, 39.
- (11) (a) Wu, L.; Chen, X. L.; Xu, Y. P.; Sun, Y. P. *Inorg. Chem.* **2006**, *45*, 3042. (b) He, M.; Chen, X. L.; Sun, Y. P.; Liu, J.; Zhao, J.; Duan, C. *Cryst. Growth Des.* **2007**, *7*, 199. (c) He, M.; Li, H.; Chen, X. L.; Xu, Y. P.; Xu, T. *Acta Crystallogr. C* **2001**, *57*, 1010.
- (12) (a) Dewey, C. F.; Cook, W. R.; Hodgson, R. J.; Wynne, J. J. *Appl. Phys. Lett.* **1975**, *26*, 714. (b) Kato, K. *Opt. Commun.* **1976**, *19*, 332. (c) Kato, K. *Appl. Phys. Lett.* **1976**, *30*, 583. (d) Stickel, R. E.; Dunning, F. B. *Appl. Opt.* **1978**, *17*, 981.
- (13) (a) Yuan, G.; Xue, D. *Acta Cryst. B* **2007**, *63*, 353. (b) Xue, D.; Betzler, K.; Hesse, H. *Appl. Phys. A: Mater. Sci. Process.* **2002**, *74*, 779. (c) Yu, D.; Xue, D. *Acta Cryst. B* **2006**, *62*, 702.
- (14) Zhang, G. C.; Liu, Z. L.; Zhang, J. X.; Fan, F. D.; Liu, Y. C.; Fu, P. Z. *Cryst. Growth Des.* **2009**, *9*, 3137.
- (15) Sasaki, T.; Mori, Y.; Yoshiura, M.; Yap, Y. K.; Kamimura, T. *Mater. Sci. Eng. R: Rep.* **2000**, *30*, 1.
- (16) Leonyuk, N. I.; Leonyuk, L. I. *Prog. Cryst. Growth Charact.* **1995**, *31*, 179.
- (17) (a) Fan, X. Y.; Pan, S. L.; Hou, X. L.; Liu, G.; Wang, J. D. *Inorg. Chem.* **2009**, *48*, 4806. (b) Wang, Y. J.; Pan, S. L.; Hou, X. L.; Zhou, Z. X.; Liu, G.; Wang, J. D.; Jia, D. Z. *Inorg. Chem.* **2009**, *48*, 7800. (c) Li, F.; Pan, S. L.; Hou, X. L.; Yao, J. *Cryst. Growth Des.* **2009**, *9*, 4091. (d) Fan, X. Y.; Pan, S. L.; Hou, X. L.; Tian, X. L.; Han, J.; Haag, J.; Poepplmeier, K. R. *Cryst. Growth Des.* **2010**, *10*, 252.
- (18) Paul, A. K.; Sachidananda, K.; Natarajan, S. *Cryst. Growth Des.* **2010**, *10*, 456.
- (19) Jesudurai, J. G. M.; Prabha, K.; Christy, P. D.; Madhavan, J.; Sagayaraj, P. *Spectrochim. Acta A* **2008**, *71*, 1371.
- (20) (a) Whatmore, R. W.; Shorrocks, N. M.; O'Hara, C.; Ainger, F. W.; Young, I. M. *Electron. Lett.* **1981**, *17*, 11. (b) Ogorodnikov, I. N.; Yakovlev, V. Y.; Isaenko, L. I. *Radiat. Meas.* **2004**, *38*, 659.
- (21) Li, R. K.; Chen, P. *Acta Crystallogr. C* **2010**, *66*, 7.
- (22) SAINT-Plus, version 6.02A; Bruker Analytical X-ray Instruments, Inc.: Madison, WI, 2000.
- (23) Sheldrick, G. M. *SHELXTL*, version 6.14; Bruker Analytical X-ray Instruments, Inc.: Madison, WI, 2003.
- (24) Sheldrick, G. M. *SHELXS-97*, Program for X-ray Crystal Structure Solution; University of Göttingen: Göttingen, Germany, 1997.
- (25) Spek, A. L. *J. Appl. Crystallogr.* **2003**, *36*, 7.
- (26) (a) Kurtz, S. Q.; Perry, T. T. *J. Appl. Phys.* **1968**, *39*, 3798. (b) Dougherty, J. P.; Kurtz, S. K. *J. Appl. Crystallogr.* **1976**, *9*, 145.
- (27) Brown, I. D.; Altermatt, D. *Acta Crystallogr. B* **1985**, *41*, 244.
- (28) Brese, N. E.; O'Keeffe, M. *Acta Crystallogr. B* **1991**, *47*, 192.
- (29) Li, J.; Xia, S.; Gao, S. *Spectrochim. Acta A* **1995**, *51*, 519.
- (30) Ross, S. D. In *The Infrared Spectra of Minerals*; Farmer, V. C., Ed.; Mineralogical Society of Great Britain and Ireland: Middlesex, U.K., 1974; p 205.
- (31) Liu, Z.; Li, S.; Zuo, C. *Thermochim. Acta* **2005**, *433*, 196.
- (32) Adamiv, V. T.; Burak, Ya. V.; Romanyuk, M. M.; Romanyuk, G. M.; Teslyuk, I. M. *Ferroelectrics* **2005**, *316*, 147.
- (33) Chen, C. T.; Wu, Y. C.; Li, R. C. *J. Cryst. Growth* **1990**, *99*, 790.
- (34) (a) Wu, Y. C.; Chen, C. T. *Acta Phys. Sin.* **1986**, *35*, 1. (b) Liu, H. X.; Liang, Y. X.; Jiang, X. J. *Solid State Chem.* **2008**, *181*, 3243.